WORKING PAPERS

N° 16-711

October 2016

"A Stochastic Model for Cytotoxis T. Lymphocyte Interaction with Tumors Nodules"

Patrick Cattiaux, Claire Christophe and Sébastien Gadat

Toulouse School of Economics

A STOCHASTIC MODEL FOR CYTOTOXIC T. LYMPHOCYTE INTERACTION WITH TUMOR NODULES.

PATRICK CATTIAUX ♠ , **CLAIRE CHRISTOPHE** ♢, AND **SÉBASTIEN GADAT** ♠

♠ Université de Toulouse

♢ Université de Nantes

Abstract. CTL (Cytotoxic T. Lymphocytes) destroy virally infected cells and tumor cells via the secretion of lytic molecules stored in intracellular granules. They are key components of the anti-cancer immune response and it is therefore crucial to study in depth, and possibly enhance, their biological responses against tumors. In [CMR$^+$15], we introduced a stochastic dynamical model that involves interacting particles based on experimentally measured parameters. It therefore makes it possible to describe CTL function during immuno-editing. At the same time, we showed on simulations that a bias in CTL motility inducing a progressive attraction towards a few scout CTL, which have detected the nodule, enhances early productive collisions and drastically improves the tumor eradication rate. In the present paper, we introduce a continuous time similar model and derive rigorously formulas for the evolution of the system CTL/Nodule. Numerical schemes then confirm the quantitative role of the bias in the CTL movement induced by scout CTL, and open new perspectives on chemotaxis for immunotherapy.

Key words : self-interacting diffusion processes, hitting time, chemotaxis .

MSC 2010 : 60J60, 60K35, 92C42

1. Introduction

The biological setting of this paper is inspired from the recent contribution [CMR$^+$15] that describes a situation where a tumor mass is confronted to an immune response. Even if the ability of the CTL to destroy a tumor single cell is proved [DL10, CFP$^+$09], in the framework of [CMR$^+$15], the existence of a gathered tumor mass circumvents immune recognition [SOS11], via the immuno-editing process. Another reason of the CTL inefficiency versus a tumor nodule, which is highlighted in [CMR$^+$15], is the accessibility of the CTL to the nodule: this accessibility highly depends on CTL displacements.

To bypass this latter difficulty, an immunotherapy is proposed in [CMR$^+$15], this strategy relies on a synergy created among CTL through chemotaxis. This therapy consists in generating CTL that are able to release chemo-attractant, when they are in contact with a tumor cell. This induces a stronger attraction of the remaining CTL towards the nodule and then improve the accessibility of the tumor. The fact that such a method will naively improve therapeutic results is not an unexpected result. However, what is important is the ratio between the very small size of the bias induced by the chemo-attraction and its therapeutic impact, suggested by the simulations in [CMR$^+$15].

Date: May 31, 2016.

To better understand the role of such an attraction, we propose here a new (deterministic) macroscopic continuous time model of a differential system describing the interaction between CTL and a tumor nodule. This macroscopic model is interpreted as the limit for a large number of interacting particles in a stochastic model, that is, the macroscopic model is derived from the microscopic point of view with an individual-centered model. We stress the fact that at the present stage this derivation is not fully rigorous from the mathematical point of view, but we explain at each step why it is plausible.

Let us briefly describe more informally the subject of our study. Because of the large number of tumor cells, we are led to consider a deterministic development of the tumor mass, which is the "mean evolution" of the probabilistic growth model developed in [CMR$^+$15]. The equation describing the growth, comes from a random microscopic model. The growth depends on the number of tumor cells that are actively dividing. We assume that the decrease of the nodule only relies on the number of CTL on the nodule border, those called *Scout CTL*. This last number is described by studying the (random) hitting time of the nodule by a free CTL, which depends on the CTL displacement model. Under some scaling assumptions, one can approximate the distribution of the position of non scout CTL by a Quasi-Stationnary-Distribution associated to the non-absorption at the boundary of the nodule.

Our model will address alternatively two different CTL displacements: one will describe a self-governing displacement and the other one will introduce a biased displacement toward the nodule. The first one is related to independent Brownian dynamics while the second one is a new kind of "reinforced" Ornstein-Uhlenbeck process. The later process is a non linear diffusion process with a linear drift reinforced at each time by the probability to hit the nodule border. The mathematics of this very natural process have to be rigorously performed, but it appears as some mean-field particles limit in the propagation of chaos regime.

Actually, some other dynamics may also fit some biological observations in a different setting. Indeed, one can better imagine that the basic dynamics is more like some "run and tumble" model (see, *e.g.*, [WL10]) or a piecewise deterministic (Markov) process as introduced in [HBC$^+$12a] for the modelization of CD8+ T cells. Nevertheless, due to the fact that some properties of hitting times are better understood in the Brownian like situation, we shall numerically test our model with the two dynamics described above. The main goal is thereafter to compare the ratio of the eradication times in both situations.

Such a model relies on a few number of parameters and makes it possible to obtain an easy numerical resolution. This numerical study reveals that even a very small bias induces a drastically quicker tumor eradication. As we already said, despite the modeling of the CTL/Nodule interaction phenomenon, this numerical aspect is what is convincing. We could then imagine to develop further statistical analysis and to apply the results for personalized medicine, that is to say finding a calibration of the parameters using clinical data of individual patient to deduce a personal calibration of the immunotherapy that leads to tumor eradication. Such medical opportunity is in line with some recent advances in biology, see among other the recent work of [LYW$^+$15]. Furthermore, stricking evidences are also reported in [BdSLY$^+$15] with *in vivo* experiments that controls lymphocyte traffic through chemokines to enhance tumor immunotherapy.

2. The Mathematical model (I).

For simplicity, we shall work in dimension 2 even though an adaptation to dimension 3 would be possible, but would require more technical efforts.

We propose an idealized model of a solid tumor: the tumor nodule is then considered as a disk of center $(0,0)$ and radius R_t (at time t), consisting of three concentric shells [KTHI$^+$00], [MDP06]. We describe below more precisely these shells that are illustrated in Figure 1.

- The inert core, the grey region in Figure 1, is composed of necrotic cells (dead cells). It is a disk of radius N_t, it is also characterized by its distance to the nodule border, E_t such that $E_t + N_t = R_t$.
- The next shell, the dark green region in Figure 1, is the quiescent part. It contains alive but non-proliferative cells owing to a low nutrient and oxygen concentration. The size of this shell is denoted $(1-\delta)E_t$.
- The superficial shell, with thickness δE_t, $\delta \in]0,1]$, the light green part in Figure 1, contains enough nutrient and oxygen to maintain active cellular division. Hence, the superficial shell is constituted of proliferative cells.

The quiescent part and the proliferative part taken together are called "alive part", while the whole thickness of the alive part is E_t.
We define A_t as the number of cells in the alive part of the nodule at time t, it corresponds to the number of cells of the green parts in Figure 1. We want to understand what kind of conditions may lead to an asymptotic annealing of the alive part, or equivalently $A_t \longrightarrow 0$ as $t \longrightarrow +\infty$. Indeed, if $A_t = 0$, only necrotic cells stay in the nodule, meaning that all alive cells are eradicated. The evolution of $(A_t)_{t\geq 0}$ of course depends on the number of CTL on the border of the nodule, since these CTL are killing alive cells in the nodule.

Let us assume the number of CTL, $n_0 \geq 2$, fixed over the time (this assumption is also a simplification of the ground-truth). At time 0, all CTL are distributed independently, following a probability distribution μ_0^i. The support of μ_0^i is $\mathbb{R}^2 \backslash \overline{\mathcal{B}(0,R_0)}$.
Let Z_t^i be the position of the CTL of index i at time t. Note that some CTL are not in contact with the tumor. Those located on the boundary of the nodule are called "scout CTL" and do not move anymore. We denote by $\mathcal{L}_t^{scout}$ and L_t respectively, the set of scout CTL and the number of scout CTL, at time t. Notations are recalled in Table 1.

2.1. **Evolution of the number of alive cells in the nodule.** The evolution of the alive cells number $(A_t)_{t\geq 0}$ is governed by two processes. On one hand, the tumor cells in the proliferative part can duplicate (create new cells) independently with the same rate λ, provided they are not in contact with a CTL. On the other hand, scout CTL can kill cells on the border of the nodule with a killing rate μ. Of course, this evolution highly depends on the cytolytic activity of the scout CTL. This cytolytic activity is not well characterized and is the subject of many studies, see for instance [GMBdB14] or [Chr14] Chap.4. As there are many cells, we consider a deterministic evolution in accordance with the Law of Large Numbers, that only takes into account some "mean evolution". However we still denote by A_t the *mean number* of alive cells. In the sequel we assume the following:

(1) Firstly, a CTL can kill one target cell at a time. In this paper, we work in continuous time. It allows us to consider simultaneous killing as very close sequential killing. This is in accordance with biological observations [RMJM78, PB82, WDFV06].
(2) Secondly, we suppose that a CTL can kill an infinite number of tumor cells, meaning that a CTL does not die and its efficiency all along the process remains constant. We shall come back below to this assumption.

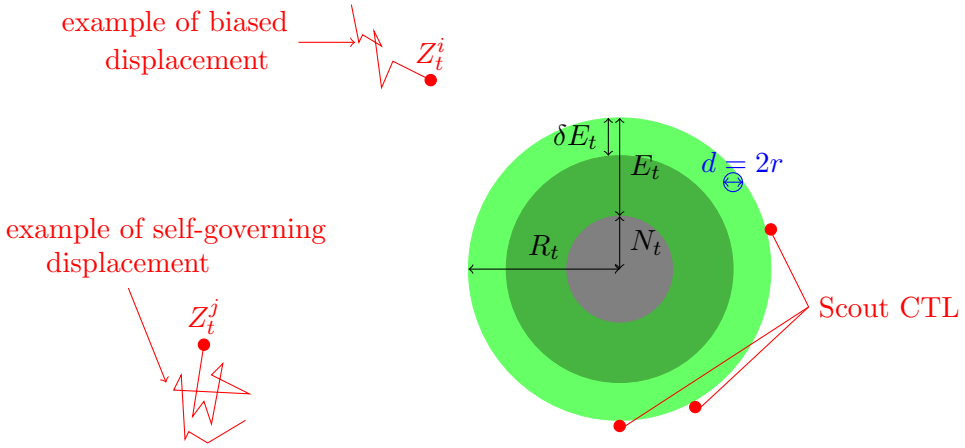

FIGURE 1. **Representation of the interaction between CTL and tumor nodule.** The *gray* region is the necrotic part, the *dark green* region is the quiescent part (alive but non-proliferative cells), and the *green shell* is the proliferative part. The *red* dots are CTL, and red lines some examples of possible trajectories before the time t.

(3) Thirdly, we assume that if a CTL is a scout CTL (touching the nodule), it is a scout CTL for the rest of the time. Indeed, when a scout CTL kills one tumor cell, the CTL stays very close to the nodule, so that it has a large probability to touch another target cell almost instantaneously, so that this CTL remains a scout CTL.

Under these conditions the number of cells in the alive part (recall alive part contains proliferative and quiescent cells), at time $t+h$, can be described by the following equation:

$$A_{t+h} = A_t + h \times \underbrace{\lambda\left(\delta A_t - \mathbb{E}(L_t)\right)\mathbb{1}_{\delta A_t - \mathbb{E}(L_t)\geq 0}}_{\text{Rate of duplication}\times\text{Number of alive cells not touched by a CTL}} - h \times \underbrace{\mu\mathbb{E}(L_t)}_{\text{Rate of killing}\times\text{Number of alive cells touched by a CTL}} + o(h).$$

This evolution equation is very natural and comes from the following justification. The (mean) number of alive cells at time $t+h$, denoted A_{t+h}, is equal to the same number at time t A_t, plus tumor cells created and minus tumor cells killed by CTL, in the short time interval $[t, t+h[$. As a CTL kills one target cell during this short time interval, the number of killed cells is equal to the mean number of scout CTL $\mathbb{E}(L_t)$, multiplied by the killing rate μ.
The tumor cells that can duplicate (create new cells) are cells in the proliferative part which are not in contact with a CTL. As a CTL kills one cell at a time, this mean number is $\delta A_t - \mathbb{E}(L_t)$. Multiplying this number by the division rate of one tumor cell λ, we obtain the then deduce that the mean number of created cells during the short time interval is $h \times \lambda \times (\delta A_t - \mathbb{E}(L_t))$.

Remark 2.1. At this macroscopic level, we should introduce several modifications in (2.1).

- Assuming that L_t tumor cells are touched by a CTL is a simplification. Indeed, we neglect the fact that one tumor cell can be touched by several immune cells. We also consider the fact that only tumor cells close to the nodule border can be touched by a CTL.

- Assuming that δA_t is the proliferative tumor cells number, is also a simplification. Indeed, the alive part is defined by its thickness E_t. Then, adding a new cell in the alive part may push another cell into the necrotic part. It should thus be possible to modify λ, multiplying it by a factor $1-\varepsilon$, and introduce $N_{t+h} = N_t + \varepsilon\lambda h\, A_t$ for the evolution of the necrotic part. In a sense, such an additionnal consideration will not really modify the mathematical study since we are only interested in the evolution of A_t. We shall neglect this aspect.
- More importantly seems to be our assumption on the infinite lifetime of the scout CTL. Again at our macroscopic level, we should assume that a constant part of the scout CTL can die or simply can become inefficient. This will therefore simply modify μ, or if we admit in addition that the proximity of a dead scout CTL does not more affect the neighboring tumor cells, it is enough to replace L_t by $(1-\varepsilon')L_t$. One more time, this modification will not really spoil the mathematical study.

$\diamondsuit$

The continuous time dynamics of A_t we propose, derived from (2.1), is thus given by:

$$\partial_t A_t = \left[\lambda(\delta A_t - \mathbb{E}(L_t))\mathbb{1}_{\delta A_t - \mathbb{E}(L_t)>0} - \mu\mathbb{E}(L_t)\right]\mathbb{1}_{A_t>0}. \tag{2.2}$$

2.2. **Equation for the radius of the nodule at time t.** In order to describe the evolution of the radius of the tumor mass, we may consider tumor cells as small disks. We thus have to face a packing problem. There exist some studies on the packing problem for small spheres into a bigger one [GLNÖ98]. In our framework however, tumor cells adapt their shape in order to be in their whole, as compact as possible. We can thus neglect the (difficult) geometrical aspect induced by the packing issue and approximate the surface occupied by alive cells, by the difference between the whole nodule area and the necrotic part area. By using a rough approximation of the tumor cell shape as a disk of radius r, we deduce that:

$$\pi r^2 A_t = \pi R_t^2 - \pi N_t^2. \tag{2.3}$$

Until now, no information is available on the behavior of the radius N_t of the necrotic part. However, two phases describe the nodule evolution: an increasing phase and a decreasing phase. During the decreasing phase of the nodule, one can suppose that the necrotic part is constant, $N_t = N$, since dead tumor cells in the necrotic part, fortunately, do not come back to life. On the contrary, during the increasing phase of the nodule, and assuming that the nodule is large enough so that nutrient and oxygen cannot go deep inside the nodule, then $E_t = E$ is constant. Alive cells far from the nodule border, become necrotic cells and N_t increases.
These two behaviors are described in Figure 2.

Therefore, Equation (2.3) becomes:

- Decreasing phase. In this case, we use $\pi R_t^2 - \pi N^2 = \pi r^2 A_t$, so that $R_t = \sqrt{r^2 A_t + N^2}$. Using Equation (2.2) and that N is constant, one obtains the following ordinary differential equation on the nodule size R_t:

$$\partial_t R_t = \left[\left(\frac{\lambda\delta R_t}{2} - \frac{\lambda\delta N^2}{2R_t} - \frac{r^2\lambda\mathbb{E}(L_t)}{2R_t}\right)\mathbb{1}_{\delta(R_t^2-N^2)-r^2\mathbb{E}(L_t)>0} - \frac{r^2\mu\mathbb{E}(L_t)}{2R_t}\right]\mathbb{1}_{R_t'<0,\ R_t>N}. \tag{2.4}$$

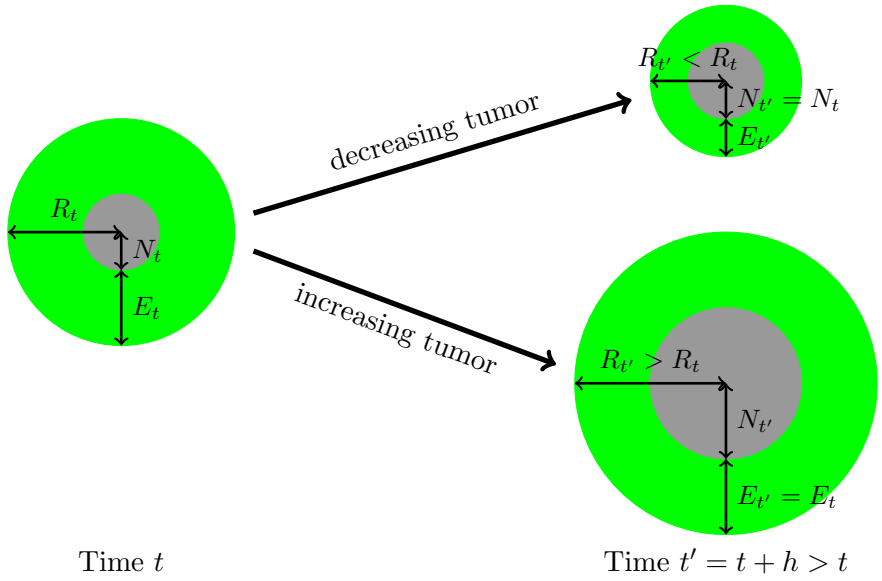

FIGURE 2. **The two dynamics of the nodule**. The green region is the alive part, and the gray region is the necrotic part of the nodule. Left: situation at time t. Top right: diminution of R_t and E_t when the tumor decreases, while N_t is constant. Down right: augmentation of R_t and N_t while E_t is constant when the tumor increases.

- Increasing phase. We still use $\pi R_t^2 - \pi(R_t - E)^2 = \pi r^2 A_t$ but in that case, E remains constant. Hence, $R_t = \frac{r^2 A_t + E^2}{2E}$ and Equation (2.2) yields:

$$\partial_t R_t = \left[\left(\lambda\delta R_t - \frac{\lambda\delta E}{2} - \frac{r^2\lambda\mathbb{E}(L_t)}{2E}\right)\mathbb{1}_{\delta(2R_tE-E^2)-r^2\mathbb{E}(L_t)>0} - \frac{r^2\mu\mathbb{E}(L_t)}{2E}\right]\mathbb{1}_{R_t'>0}. \tag{2.5}$$

We collect for the reader convenience in Table 1 all notations we already introduced and will use in the sequel.

2.3. **Number of CTL on the border of the nodule.** Recall that scout CTL are CTL on the border of the nodule, i.e. at time t, the number of scout CTL (for $|.|$ a given norm in $\mathbb{R}^2$) satisfies the equation

$$L_t = \sum_{i=1}^{n_0} \mathbb{1}_{|Z_t^i| \le R_t}. \tag{2.6}$$

We shall now derive an equation for the dynamics of $\mathbb{E}(L_t)$. It is clear that we have to evaluate the hitting time by Z_t of the centered ball with radius R_t. Even for very standard dynamics of stochastic particles, the behavior of such a hitting time is delicate, even more here since R_t depends on the time and the whole past of the particles $Z_\cdot^i$.

In all what follows we assume that the dynamics of each CTL is given by a strong Markov process.

Variable	Description
R_t	nodule radius at time t
E_t	alive part thickness of the nodule at time t
N_t	necrotic part radius of the nodule at time t
A_t	number or mean number of alive cells (quiescent cells and proliferative cells) at time t
μ_0^i	initial distribution of the CTL i
$\mu_t^i = \mu_t$	distribution of the CTL i at time t
$\mathcal{L}_t^{scout}$	set of scout CTL (CTL touching the nodule) at time t
L_t	number of scout CTL at time t
Z_t^i	position of the CTL i at time t
Parameter	**Description**
n_0	CTL number
δ	proliferative part proportion in the alive part
μ	killing rate
λ	division rate of one tumor cell
d	tumor cell diameter
r	tumor cell radius

TABLE 1. Variables and parameters used in the model

As before we study the variation of L_t on a small time interval. For $h > 0$, the number of scout CTL at time $t + h$ is equal to the number of scout CTL at time t (recall that a scout CTL remains a scout CTL), plus the number of non-scout CTL that reach the nodule between times t and $t + h$. Formally

$$\text{card}\left\{i, \quad Z_t^i \notin \mathcal{L}_t^{scout} \text{ and } \exists\ 0 < s \leq h,\ |Z_{t+s}^i| \leq R_{t+s}\right\}.$$

However, for h small, on $]t, t+h[$, the nodule radius shall not vary too much (tumor cell division rate is small, see Table 2 for some realistic orders of magnitude of the several parameters). Thus, we may assume that $R_{t+s} = R_t$ on this small time interval. One thus get the following equation

$$\begin{aligned} L_{t+h} &= L_t + \sum_{i|Z_t^i \notin \mathcal{L}_t^{scout}} \mathbb{1}_{\min_{0\leq s\leq h}\ |Z_{t+s}^i| \leq R_t} \\ &= L_t + \sum_{i=1}^{n_0} \mathbb{1}_{\left\{Z_{t+h}^i \in \mathcal{L}_t\right\} \cap \left\{Z_t^i \notin \mathcal{L}_t^{scout}\right\}}. \end{aligned}$$

Recall that we assume that the motion of all CTL are independent and that the initial distributions are i.i.d. Hence the distributions of the CTL at time t are still i.i.d. Define for $i \leq n_0$ and $A \subset \mathbb{R}^2 \backslash \overline{\mathcal{B}(0, R_t)}$,

$$\mu_t^i(A) = \mathbb{P}_{\mu_0^i}(Z_t^i \in A | |Z_t^i| > R_t).$$

We thus have,

$$\begin{aligned} \mathbb{E}(L_{t+h}) &= \mathbb{E}(L_t) + \mathbb{E}\left(\sum_{i=1}^{n_0} \mathbb{1}_{\left\{Z_{t+h}^i \in \mathcal{L}_t^{scout}\right\} \cap \left\{Z_t^i \notin \mathcal{L}_t^{scout}\right\}}\right) \\ &= \mathbb{E}(L_t) + n_0\, \mathbb{P}\left(Z_{t+h}^1 \in \mathcal{L}_t^{scout} | Z_t^1 \notin \mathcal{L}_t^{scout}\right)\, \mathbb{P}\left(Z_t^1 \notin \mathcal{L}_t^{scout}\right), \end{aligned}$$

as the trajectories are assumed identically distributed. Hence, using the Markov property

$$\mathbb{E}(L_{t+h}) = \mathbb{E}(L_t) + n_0\, \mathbb{P}\left(Z_t^1 \notin \mathcal{L}_t^{scout}\right)\, \mathbb{P}_{\mu_t}\left(\tau_{R_t}^1 \leq h\right),$$

where $\tau_{R_t}^1 = \inf\left\{s > 0, \ \ |Z_{t+s}^1| \leq R_t\right\}$ is the hitting time of R_t by Z_t^1.

Note that

$$\mathbb{P}(Z_t^1 \in \mathcal{L}_t^{scout}) = \frac{1}{n_0} \sum_{i=1}^{n_0} \mathbb{E}\left(\mathbb{1}_{Z_t^i \in \mathcal{L}_t^{scout}}\right) = \frac{1}{n_0}\,\mathbb{E}(L_t).$$

Hence,

$$\mathbb{E}(L_{t+h}) = \mathbb{E}(L_t) + (n_0 - \mathbb{E}(L_t))\,\mathbb{P}_{\mu_t}\left(\tau^1_{R_t} \leq h\right). \tag{2.7}$$

Thus we arrive at the following continuous time model:

$$\partial_t \mathbb{E}(L_t) = (n_0 - \mathbb{E}(L_t))\,\lim_{h\to 0} \frac{\mathbb{P}_{\mu_t}(\tau^1_{R_t} \leq h)}{h}. \tag{2.8}$$

2.4. **CTL dynamics.** In order to extend our investigations, we have to describe the CTL dynamics. In the next section, we will study the previous system of Equations (2.8) and (2.4)/(2.5) for two dynamical models.

First, a self-governing CTL displacement is studied. Indeed, it is not known if immune cells are attracted by the nodule without immunotherapy. In addition, interactions between CTL are not established. In [HBC$^+$12b] independent generalized Lévy random walks are suggested for CTL motility in brain. For the sake of simplicity, we shall here assume independent Brownian motions for CTL dynamics.

Second, CTL displacement under simulated immunotherapy is introduced. As suggested in [CMR$^+$15], this therapy consists in the generation of CTL that can release chemo-attractants when they are scout CTL and this model is supported by the recent biological works of [BdSLY$^+$15]. Keeping in mind that the free motility is given by a Brownian motion, we assume a time dependent Ornstein-Uhlenbeck (O.U.) dynamics for CTL motility. Time dependence here will be introduced in the linear coefficient of the drift term which will depend on the number of scout CTL (hence will increase in our model).

3. Hitting time and number of scout CTL.

Let us assume that t is fixed in this Section. In this part, we obtain an explicit expression of the main term of (2.8), that is an expression for:

$$\lim_{h\to 0} \frac{\mathbb{P}_{\mu_t}(\tau^1_{R_t} \leq h)}{h}.$$

3.1. **Brownian dynamics.** In this subsection, let us assume that the dynamics of non-scout CTL are independent Brownian motions. This suggests that CTL do not preferentially direct towards a developing tumor. Let Z_{t+s} be the position of a non-scout CTL at time $t+s$. For $0 \leq s$, it satisfies

$$\mathrm{d}Z_{t+s} = \sigma\ \mathrm{d}B_s$$

up to the first time it reaches the nodule's boundary, with an initial distribution at time t given by μ_t. Up to a time change we may assume that $\sigma = 1$, but for later purpose we keep in mind that the Brownian motion variance can be chosen arbitrarily.

Remember that τ_{R_t} is the first time for a non-scout CTL to hit the nodule, i.e. the first time the norm $\rho_s = ||Z_{t+s}||_2$ of the process equals R_t:

$$\tau_{R_t} := \inf\{s + t \geq t \,:\, \|Z_{s+t}\|_2 \leq R_t\}\,.$$

Recall that the radial part of a $2-D$ Brownian motion is a Bessel process, i.e. $\rho_\cdot$ solves the following stochastic differential equation:

$$\left\{ \begin{array}{l} \mathrm{d}\rho_s = \mathrm{d}B_s + \frac{1}{2\rho_s}\,\mathrm{d}s \\ \rho_0 = ||Z_t||_2 > R_t \end{array} \right. . \tag{3.1}$$

Of course the problem here is that the size of the nodule is changing with the time, i.e. we are looking at some Bessel process up to the hitting time of a moving boundary. Explicit results for this kind of problem are not known, but since we are looking at the probability for this hitting time to be close to 0, up to a second order error we may assume that $R_{t+s} = R_t$ for $s \leq h$ and small h. In this situation, the distribution of τ_{R_t} starting from a given initial point is known, see for instance [RY99, BS02, HM13, BMR13]. More precisely, using the results in [BMR13] and the scaling properties of the Brownian motion

$$\mathbb{P}_x(\tau_{_R} \leq h) = \mathbb{P}_{x/R}(\tau_{_1} \leq (h/R^2)) = \tag{3.2}$$

$$= \int_0^{h/R^2} C(|x|/R)\,\frac{|x|-R}{|x|\,s^{\frac{3}{2}}}\;e^{-\frac{(|x|-R)^2}{2sR^2}}\,\frac{\left(\frac{|x|}{R}+s\right)^{\frac{1}{2}}\,(1+\ln(|x|/R))}{(1+\ln(s+|x|/R))\,(1+\ln(1+\ln(s+|x|/R)))}\,ds\,.$$

where $z \mapsto C(z)$ is bounded on $]1,+\infty[$. Since we now start from some initial distribution μ_t and only look at small time h, it is not too difficult to see that the limiting value $C(1) = \lim_{z\to 1} C(z)$ is important and that the behavior of μ_t near the boundary of the module is crucial. Let us state the first main result.

Theorem 3.1. *Let $\mu(\,\mathrm{d}x) = f(x)\,\mathrm{d}x$ be an absolutely continuous probability distribution supported by $|x| > R$. Assume that $f(x) = 0$ for $|x| = R$. Denote by g the radial part of the density f and assume that g is differentiable in a neighborhood of R, then*

$$\lim_{h\to 0} \frac{\mathbb{P}_\mu(\tau_{_R} < h)}{h} = \frac{g'(R)}{2}.$$

Sketch of proof.
We first give a somehow formal proof starting with (3.2). First of all, it is easy to see that for $\alpha < \frac{1}{2}$,

$$\mathbb{P}_\mu(\tau_{_R} \leq h) = \int_{R<|x|<R+h^\alpha} \mathbb{P}_x(\tau_{_R} \leq h)\,f(x)\,dx + o(h)\,.$$

Next we have

$$\mathbb{P}_\mu(\tau_{_R} \leq h) = C(1)\int_{R<|x|<R+h^\alpha}\int_0^{h/R^2} \frac{|x|-R}{R\,s^{\frac{3}{2}}}\;e^{-\frac{(|x|-R)^2}{2sR^2}}\,f(x)\,ds\,dx\; + o(h)\,,$$

provided $C(z)$ admits a limit as $z \to 1$ (that we do not know in whole rigor). A simple change of variables and then integration by parts (using $g(R) = 0$) yield

$$\begin{aligned} \mathbb{P}_\mu(\tau_{_R} \leq h) &= C'(1)\int_{0<u<h^\alpha}\int_0^{h/R^2} \frac{u}{R\,s^{\frac{3}{2}}}\;e^{-\frac{u^2}{2sR^2}}\,g(R+u)\,ds\,du\; + o(h) \\ &= C'(1)\int_{0<u<h^\alpha}\int_0^{h/R^2} \frac{R^2}{R\,s^{\frac{1}{2}}}\;e^{-\frac{u^2}{2sR^2}}\,g'(R+u)\,ds\,du\; + o(h)\,. \end{aligned}$$

But

$$\int_{0<u<h^\alpha} \frac{1}{R\, s^{\frac{1}{2}}}\, e^{-\frac{u^2}{2sR^2}}\, g'(R+u)\, du \;\to\; C\, g'(R)$$

as $s \to 0$, where C is a normalizing constant obtained after the Laplace method in the previous integral. Then, the Lebesgue's bounded convergence theorem leads to:

$$\lim_{h\to 0} \frac{\mathbb{P}_\mu(\tau_{_R} \leq h)}{h} = C''\, g'(R)\,.$$

□

This proof is not fully rigorous since we assumed some unknown (but plausible) property for $C(z)$ and does not furnish the exact value of the constant C''.

That is why we shall give later another proof, simply using comparison theorems for one dimensional stochastic differential equations ([IW81, p 438]), which furnishes $C'' = \frac{1}{2}$. This comparison method then can be generalized to more sophisticated dynamics as the Ornstein Uhlenbeck dynamics (see Theorem 3.3 below).

How can we apply the previous theorem to our model ? Let μ_t be the probability distribution of one CTL at time t, conditioned not to be a scout CTL. We claim that μ_t is absolutely continuous with respect to the Lebesgue measure, so that $\mu_t(\,\mathrm{d}x) = f_t(x)\,\mathrm{d}x$, $f_t(x) = 0$ for $|x| = R_t$ and f_t is smooth on $|x| > R_t$.
Indeed, up to a deterministic function of t, it is enough to show these properties for the measure

$$h \mapsto \mathbb{E}(h(Z_t)\, \mathbb{1}_{\tau_{_{R_t}} > t})\,.$$

This can be shown by using the (partial) Malliavin calculus techniques of [Cat87, Cat91] for the second coordinate of the process $t \mapsto (R_t, Z_t)$. In addition, looking at $(R_t, \rho_t - R_t)$ up to the first hitting time of 0 by the second coordinate, we can similarly prove that the radial part of this density is C^1 up to $|y| = R_t$. Of course since the support of g_t is $[R_t, +\infty[$ and $g_t(R_t) = 0$ we have $g_t'(R_t) \geq 0$.

We thus will obtain the next result.

Theorem 3.2. *Let $\mu_t(\,\mathrm{d}x) = f_t(x)\,\mathrm{d}x$ be the probability distribution of one CTL at time t, conditioned not to be a scout CTL. g_t will denote the density of the distribution of the radial part of μ_t. Then*

$$\partial_t \mathbb{E}(L_t) = (n_0 - \mathbb{E}(L_t))\, \lim_{h\to 0} \frac{\mathbb{P}_{\mu_t}(\tau_{_{R_t}} < h)}{h} = (n_0 - \mathbb{E}(L_t))\, \frac{g_t'(R_t)}{2}.$$

Actually we shall prove a more general result:

Theorem 3.3. *Consider $(B_t)_{t\geq 0}$ a Brownian motion with respect to a filtration $(\mathcal{F}_t)_{t\geq 0}$ and $(b_s)_{s\geq 0}$ a locally bounded function such that for any $s \geq 0$: b_s is $\mathcal{F}_s$ measurable. We define some general drifted linear Brownian motion as:*

$$u_t = u_0 + B_t + \int_0^t b_s\,\mathrm{d}s,$$

where $t \longmapsto R_t$ is a C^1 moving boundary such that $R_0 < u_0$. We assume that μ the distribution of u_0 has a (locally bounded) density g w.r.t. the Lebesgue measure such that $g(R_0) = 0$ and $g'(R_0)$ exists. Then

$$\lim_{h\longrightarrow 0} \frac{\mathbb{P}_\mu(\tau_{_{R_t}} < h)}{h} = \frac{g'(R_0)}{2}\,.$$

Proof. Step 1. From a moving boundary to a fixed one.
Consider a C^1 moving boundary R_t such that $u_0 > R_0$ and a one dimensional drifted Brownian motion

$$u_t = u_0 + B_t + \int_0^t b_s \, \mathrm{d}s.$$

The hitting time we are looking for τ_{R_t} is such that $u_t = R_t$. Writing $v_t = u_t - R_t$, τ_{R_t} is simply the first time the process $v_\cdot$ reaches 0. That is, replacing b_t by $b_t - R'_t$, we may replace the moving boundary by a fixed one located at point 0. ◇

Step 2. The case without drift.
Here we thus consider a linear Brownian motion starting with an initial distribution $\mu(\mathrm{d}v) = g(v)\,\mathrm{d}v$ supported by $]0, +\infty[$ with $g(0) = 0$, and such that $g'(0)$ exists (and is obviously non-negative). We want to estimate $\mathbb{P}_\mu(\tau_0 < h)/h$.
In this case, the distribution of τ_0 is explicitly known and is given by:

$$\mathbb{P}_\mu(\tau_0 < h) = \int_0^{+\infty} \int_0^h \frac{v}{\sqrt{2\pi\, s^3}}\, e^{-\frac{v^2}{2s}}\, \mathrm{d}s\, \mu(\mathrm{d}v)\,.$$

We split the integral in $\mathrm{d}v$ into two parts: from 0 up to $\sqrt{2h\,\ln(1/h)}$ and from $\sqrt{2h\,\ln(1/h)}$ up to $+\infty$.
Let start with the second part, *i.e.*, for $v \geq \sqrt{2h\,\ln(1/h)}$ we have:

$$\begin{aligned}\int_0^h \frac{v}{\sqrt{2\pi\, s^3}}\, e^{-\frac{v^2}{2s}}\, \mathrm{d}s &= \int_{\frac{v^2}{2h}}^{+\infty} e^{-u}\,(\pi\, u)^{-\frac{1}{2}}\, \mathrm{d}u \\ &\leq \frac{\sqrt{2h}}{v}\, e^{-v^2/2h} \leq \frac{h}{\sqrt{\ln(1/h)}} = o(h)\,.\end{aligned}$$

Hence, since μ is a probability measure, we deduce that:

$$\int_{v \geq \sqrt{2h\,\ln(1/h)}} \int_0^h \frac{v}{\sqrt{2\pi\, s^3}}\, e^{-\frac{v^2}{2s}}\, \mathrm{d}s\, \mu(\mathrm{d}v) = o(h)\,.$$

Now, a direct computation yields:

$$\begin{aligned}\int_0^{\sqrt{2h\,\ln(1/h)}} \int_0^h \frac{v}{\sqrt{2\pi\, s^3}}\, e^{-\frac{v^2}{2s}}\, \mathrm{d}s\, g(v)\, \mathrm{d}v &= \int_0^{\sqrt{2h\,\ln(1/h)}} \int_{\frac{v^2}{2h}}^{+\infty} e^{-u}\,(\pi\, u)^{-\frac{1}{2}}\, \mathrm{d}u\, g(v)\, \mathrm{d}v \\ &= \int_0^{+\infty} \frac{e^{-u}}{\sqrt{\pi\, u}} \int_0^{\sqrt{2h(u \wedge \ln(1/h))}} g(v)\, \mathrm{d}v\, \mathrm{d}u\,.\end{aligned}$$

We split the last integral according to the values of u. Since $g(0) = 0$, a first order Taylor expansion leads to $g(v) = vg'(0) + v\varepsilon$ for all $v \leq \sqrt{2h\ln(1/h)}$ and some ε going to 0 with h. We then deduce that:

$$\int_{\ln(1/h)}^{+\infty} \frac{e^{-u}}{\sqrt{\pi\, u}} \int_0^{\sqrt{2h\ln(1/h)}} g(v)\, \mathrm{d}v\, \mathrm{d}u \leq h^2\, \ln^{3/2}(1/h)(g(0) + \varepsilon) = o(h)\,.$$

Next

$$\begin{aligned}\int_0^{\ln(1/h)} \frac{e^{-u}}{\sqrt{\pi\, u}} \int_0^{\sqrt{2hu}} g(v)\, \mathrm{d}v\, \mathrm{d}u &= h\, \frac{g'(0)+\varepsilon}{\sqrt{\pi}} \int_0^{\ln(1/h)} e^{-u}\, \sqrt{u}\, \mathrm{d}u \\ &= h\, \frac{g'(0)+\varepsilon}{\sqrt{\pi}} \left(\int_0^{+\infty} e^{-u}\, \sqrt{u}\, \mathrm{d}u + O(h \ln^{1/2}(1/h)) \right) \\ &= h\, \frac{g'(0)}{2} + o(h)\,.\end{aligned}$$

We then obtain the conclusion of the proof in that case. ◇

Step 3. Brownian motion with a constant drift.
Consider now a Brownian motion with a constant drift b. We thus have

$$\mathbb{P}_\mu(\tau_0 < h) = \int_0^{+\infty} \int_0^h e^{bv - \frac{1}{2}b^2 s}\, \frac{v}{\sqrt{2\pi\, s^3}}\, e^{-\frac{v^2}{2s}}\, \mathrm{d}s\, \mu(\mathrm{d}v)\,.$$

But similarly to the previous step, if $v \geq \sqrt{2h\ln(1/h)}$ we get an upper bound of the type $\frac{\sqrt{2}h}{v}\, e^{bv - \frac{v^2}{2h}}$. A short study of this function shows that as soon as

$$\sqrt{2h\ln(1/h)} \geq bh,$$

it is decreasing in v (for $v \geq \sqrt{2h\ln(1/h)}$ of course), so that it is less than $\frac{h}{\sqrt{\ln(1/h)}}\, e^{b\sqrt{2h\ln(1/h}} = o(h)$. Since we are integrating on $s \in [0,h]$ and for $v \leq \sqrt{2h\ln(1/h)}$ the correcting term

$$e^{bv - \frac{1}{2}b^2 s}$$

in the integral is close to 1. Hence, the result of the previous step is unchanged. In particular it does not depend on the value of b. ◇

Step 4. Drifted Brownian motion.
Assume that the drift b_t is bounded above and below by b_+ and b_- respectively. Then we have

$$B_t + b_- t \leq B_t + \int_0^t b_s\, \mathrm{d}s \leq B_t + b_+ t$$

so that it can be immediately seen that we still have the same result. Finally we can extend the result to any locally bounded drift, provided that the process is well defined. For example, we just introduce the first time the process enters the interval $[0,1]$. Indeed

$$\mathbb{P}_\mu(\tau_0 < h) = \int_{u\leq 2} \mathbb{P}_u(\tau_0 < h)\, \mu(\mathrm{d}u) + \int_{u>2} \mathbb{P}_u(\tau_0 < h)\, \mu(\mathrm{d}u)$$

and for $u > 2$, the Markov property yields

$$\mathbb{P}_u(\tau_0 < h) = \mathbb{P}_u(\tau_1 < h)\, \mathbb{P}_1(\tau_0 < h - \tau_1\,) = o(h)\,.$$

Indeed, $\mathbb{P}_1(\tau_0 < h') \leq \mathbb{P}_1(\tau_{0,2} < h')$ where $\tau_{0,2}$ denotes the exit time from the interval $[0,2]$, and since the drift is bounded on this interval the latter is $o(h)$. When $u \leq 2$ we may similarly write

$$\mathbb{P}_u(\tau_0 < h) = \mathbb{P}_u(\tau_0 = \tau_{0,3} < h) + \mathbb{P}_u(\tau_3 = \tau_{0,3} < h)\,.$$

Using $3 - u > 1$ the second term is $o(h)$, and for the first one we only have to consider the diffusion on $[0,3]$ so that the drift is bounded. These considerations permit to extend our result to the situation of locally bounded drift. ◇

Step 5. Conclusion.
The previous step can be directly used for proving Theorem 3.1 and Theorem 3.2 since the corresponding drift $b_s = 1/2\rho_s - R_s$ is bounded on any bounded time interval up to τ_0. □

Remark 3.4. *Of course the main idea behind the previous proof is that, once we have shown the result for the Brownian motion (whose instantaneous speed is of order $\sqrt{t}$ in short time) adding a drift which is locally of order bt does not change the time needed to hit the boundary.*

3.2. **Ornstein-Uhlenbeck dynamics.** In this subsection, we consider a simulated immunotherapy, such that free CTL are attracted by the scout CTL sticked on the nodule border. Formally, free CTL displacements are represented by independent Ornstein-Uhlenbeck process (O.U.). But the attracting force will increase with the number of scout CTL. Let us describe the system: we define as $\tau^i_{R_t}$ the first time the CTL i hits the boundary of the nodule. Then, the random dynamical system is described by:

$$\mathrm{d}Z^i_s = \mathrm{d}B^i_s - \nu_s Z^i_s \,\mathrm{d}s\,, \tag{3.3}$$

where ν_t is the common weight to direct Z^i_t towards the nodule.
The simplest way to introduce an increasing attracting force is to choose $\nu_t = \alpha + \beta\, L_t$ (recall that L_t is the number of scout CTL at time t):

$$\forall s \geq 0 \qquad \nu_s = \alpha + \beta\, \mathrm{card}\left\{1 \leq j \leq n_0 \,:\, |Z^i_s| \leq R_s\right\}.$$

Since the probability for two CTL to hit the nodule at the same time is equal to 0, L_t is a well defined jump process, bounded by n_0 and one can build a pathwise stochastic solution between two consecutive hitting times by two different particles, up to the final time where all CTL are scout CTL. But if n_0 is big, using exchangeability we can at a formal level, replace L_t by $\mathbb{E}(L_t)$, so that in the sequel we will assume that the particles are all *independent* and satisfy:

$$\mathrm{d}Z^i_s = \mathrm{d}B^i_s - (\alpha + \beta\mathbb{E}(L_s))Z^i_s\,\mathrm{d}s \;=\; \mathrm{d}B^i_s - (\alpha + \beta n_0\, \mathbb{P}(\tau^i_{R_\cdot} < s))\, Z^i_s\,\mathrm{d}s, \tag{3.4}$$

for some non-negative α and β up to $\tau^i_{R_\cdot}$, where $\tau^i_{R_\cdot}$ is the first time the process hits the nodule $B(0, R_\cdot)$, i.e., the first time t such that $|Z_t| = R_t$.

Actually the existence of a solution of (3.4) is still an open problem. This existence property can be shown in one dimension using monotonicity properties. In higher dimensions, it can be seen as the non linear limit of the exchangeable system of particles we described above (propagation of chaos). A discretized version, in the spirit of the Euler scheme is easy to define, and one can also hope that the continuous version can be built using this discretization scheme. Nevertheless in the sequel we shall assume existence for (3.4). The mathematical reader can thus think that the only rigorous situation is for $\beta = 0$.

As in the Brownian dynamics, the radial process $(\rho_s)_{s\geq 0}$ satisfies the following stochstic differential equation:

$$\mathrm{d}\rho_s = \mathrm{d}B'_s + \left(\frac{1}{2\rho_s} - (\alpha + \beta\mathbb{E}(L_s))\rho_s\right)\mathrm{d}s,$$

where $(B'_s)_{s\geq 0}$ is a standard one dimensional Brownian motion. Therefore, we can apply Theorem 3.3 to deduce a differential equation for $\mathbb{E}(L_t)$ provided that g_t (the density w.r.t. the Lebesgue measure at time t of μ_t) is differentiable at R_t that can be shown exactly as in the previous subsection, since $t \longmapsto \mathbb{E}(L_t)$ is C^1, using this time Malliavin calculus for time dependent coefficients as in [CM02, SSTT07] and Malliavin calculus near the boundary as in [Cat87, Cat91].

The consequence of this paragraph is that the statement of Theorem 3.2 remains unchanged for the (reinforced) Ornstein-Uhlenbeck dynamics we are proposing in Equation (3.4).

Remark 3.5. *Let us make a final remark. If we introduce a diffusion matrix $\sigma\, Id$, a simple time scale shows that if the dynamics* (3.4) *is replaced by* $\mathrm{d}Z_s^i = \sigma\,\mathrm{d}B_s^i - (\alpha + \beta\mathbb{E}(L_s))Z_s^i\,\mathrm{d}s$, *then*

$$\lim_{h\longrightarrow 0} \frac{\mathbb{P}_\mu(\tau_{R_t} < h)}{h} = \frac{\sigma^2\, g_t'(R_t)}{2}.$$

4. The mathematical model (II).

4.1. **Macroscopic model.** In this Section, we gather the several equations obtained above to obtain a macroscopic model. Below, the notation $(R_t)_{t\geq 0}$ refers to the evolution of the radius of the nodule although l_t is the mean number of scout CTL at time t. We also define h_t the radial density of μ_t, the measure of the CTL supported by $B(0,R_t)^c$. Finally, we denote $\mathcal{L}$ the infinitesimal generator of the radial part of the Markov process $(Z_t)_{t\geq 0}$ and define:

$$p_t := \mathbb{P}(\tau_{R_t} > t).$$

Consequently, p_t is the probability of not hitting the nodule before t, and satisfies the following partial differential equation $\partial_t p_t(y) = \mathcal{L}p_t(y)$. We have in mind that h_t/τ_t is the density distribution of the process conditioned not to be killed when hitting R_t. We can then summarise the macroscopic model with the following system of equations:

$$\begin{cases} \partial_t R_t = \left[\left(\lambda\delta R_t - \frac{\lambda\delta E}{2} - \frac{r^2\lambda l_t}{2E}\right)\mathbb{1}_{\delta(2R_tE-E^2)-r^2\,l_t>0} - \frac{r^2\mu l_t}{2E}\right]\mathbb{1}_{\partial_t R_t\geq 0} \\ \qquad\quad + \left[\left(\frac{\lambda\delta R_t}{2} - \frac{\lambda\delta N^2}{2R_t} - \frac{r^2\lambda l_t}{2R_t}\right)\mathbb{1}_{\delta(R_t^2-N^2)-r^2 l_t>0} - \frac{r^2\mu l_t)}{2R_t}\right]\mathbb{1}_{\partial_t R_t<0,\ R_t>N} \\ \partial_t\, l_t = (n_0 - l_t)\frac{\sigma^2\,\partial_y h_t(R_t)}{2\tau_t} \\ \partial_t h_t(y) = \mathcal{L}^* h_t(y) \text{ for } |y| > R_t \text{ and } h_t(R_t) = 0 \\ \partial_t\, p_t(y) = \mathcal{L}\, p_t(y) \text{ for } |y| > R_t \text{ and } p_t(R_t) = 0 \end{cases} \tag{4.1}$$

The initial conditions are given by R_0, $l_0 = 0$, $\tau_0 = 1$ and h_0 being a probability density. L denotes the generator of the radial part of the dynamics, *i.e.*, either

$$\mathcal{L} = \frac{1}{2}\,\sigma^2\,\partial^2_{y^2} + \frac{\sigma^2}{2y}\,\partial_y$$

in the Brownian case described by Equation (3.1), or

$$\mathcal{L} = \mathcal{L}_t = \frac{1}{2}\,\sigma^2\,\partial^2_{y^2} + \left(\frac{\sigma^2}{2y} - (\alpha + \beta l_t)y\right)\partial_y$$

in the case of the reinforced Ornstein-Uhlenbeck dynamics used in Equation (3.4). $\mathcal{L}^*$ denotes the adjoint of $\mathcal{L}$ with respect to the Lebesgue measure.

Let us make some comments on the evolution given by (4.1).

- Note that, at the beginning, the tumor nodule is growing. Since, the time $t = 0$ is assumed to be the first time of the CTL/nodule interaction with $l_0 = 0$.

- It is worth pointing out that if at time T the nodule enters in a decreasing phase, the nodule remains in a decreasing phase. Indeed, when a CTL hits the boundary of the nodule, it remains a scout CTL forever, meaning that $t \longmapsto l_t$ is an increasing function. Consequently, when $\partial_t R_t < 0$ at time T, then the terms into the brackets of the second line of (4.1) remains negative for any $t > T$.
- Consequently, when at time T the nodule is decreasing, *i.e.*, $\partial_t R_t < 0$, then the necrotic part radius is thus equal to N_T the remaining time. One can expect two different behaviors for a decreasing tumor: leading to its destruction, meaning that the alive tumor cell number equals to 0, or an equilibrium between new tumor cells obtained by division and tumor cells killed by CTL. In both cases, equilibrium or decreasing tumor mass, it is a success of the CTL response against tumor.

We do not pretend to study this system and will introduce below another simplification to push further our investigations.

4.2. **The case of high agitation of the non-scout CTL.** In this paragraph, we assume that the non-scout CTL are highly motile in comparison with the time needed for a cell to duplicate. This assumption is realistic if we consider the time scale of the considered phenomenon: the motility of a CTL is approximately 8.66 $\mu m/min$ (see [CMR$^+$15]) although the duplication of one tumor cell is of the order $10^{-3}/min$ and the killing rate of the order $4.10^{-2}/min$ as reported in Table 2. Consequently, this high motility corresponds to a large σ, *i.e.*, the natural time scale of the dynamics of the CTL is very short in comparison to the one of the nodule growth. In this situation we can accept the fact that the radial part of the distribution of the CTL conditioned not to be a scout CTL (μ_t) is almost constant, *i.e.*, is close to the Yaglom limit of the process with generator $\mathcal{L}$ if such a distribution exists. Let first recall some facts on Quasi-Stationary Distribution (QSD) and Yaglom limits. For a general view on QSD we refer to the survey [MV12] or to the monograph [CMSM13].

Let ρ be a linear (1-D) Markov process and $\tau_{_R}$ the first time it reaches R. We assume that for all starting point x, $\tau_{_R}$ is almost surely finite. We introduce the next definition.

Definition 4.1. *Let $t > 0$, $R > 0$ and μ be a probability distribution on $]R, \infty[$. The distribution μ is said to be a quasi-stationary distribution (QSD) if, for all $s \geq 0$ and any measurable set $A \subset]R, \infty[$,*

$$\mu(A) = \mathbb{P}_\mu(\rho_s \in A | \tau_{_R} > s).$$

μ is said to be a Yaglom limit if for all $x > R$ and any measurable set $A \subset]R, \infty[$, ,

$$\mu(A) = \lim_{s \to +\infty} \mathbb{P}_x(\rho_s \in A | \tau_{_R} > s).$$

A Yaglom limit is always a (QSD) but the converse is not always true.

The problem here is that, if the existence of a Yaglom limit is known for a one dimensional Ornstein-Uhlenbeck process, it does not exist for the Brownian motion on $\mathbb{R}$: the additional part of the drift $\sigma^2/2\rho$ does not play a significant role with respect to this problem. But of course we can slightly modify the model by adding another boundary condition for the dynamics of the non-scout CTL, namely assume that the corresponding process is reflected when $|z| = M$ for a large enough M ($M \gg R$). Again, this assumption seems realistic in our framework since it corresponds to a situation where the interaction CTL/nodule evolves in a compact domain. From the analytic point of view we simply add a Neumann boundary condition on $|y| = M$. Hence we consider, for the evolution of the modulus of CTL, the following reflected stochastic

differential equations, which replace either (3.1) or (3.4):

$$\begin{aligned} \mathrm{d}\rho_t &= \sigma^2\,\mathrm{d}B_t + \frac{\sigma^2}{2\rho_t}\,\mathrm{d}t + \mathrm{d}L_t^{R/2} - \mathrm{d}L_t^M \qquad \text{Brownian case} \\ &\text{or} \\ \mathrm{d}\rho_t &= \sigma^2\,\mathrm{d}B_t + \left(\frac{\sigma^2}{2\rho_t} + (\alpha+\beta\, l)\rho_t\right)\mathrm{d}t + \mathrm{d}L_t^{R/2} - \mathrm{d}L_t^M \qquad \text{Reinforced O.U. case,} \end{aligned} \tag{4.2}$$

where $L_\cdot^a$ denotes the local time of the process at a, i.e. we consider the process reflected at $R/2$ (for example) and M. We then will kill the process when hitting R, so that the reflection on the left has no importance.

The main interest is that now, the semi-group associated to the process is ultra-bounded (or ultra-contractive depending of the references) since the state space is compact. As explained in the Appendix B of [CM10], it thus follows that there exists an unique Yaglom limit and that this Yaglom limit is the quasi-limiting distribution starting from any initial distribution (no more only the Dirac masses δ_x).

One immediate consequence is the following well known result (see e.g. [CMSM13, theorem 2.2 p19]):

Theorem 4.1. *If μ is the Yaglom limit of the process $\rho_\cdot$, then there exists a positive real number θ_μ such that*

$$\mathbb{P}_\mu(\tau_{_R} > s) = e^{-\theta_\mu s}.$$

Hence

$$\lim_{h\to 0} \frac{\mathbb{P}_\mu(\tau_{_R} \le h)}{h} = \theta_\mu\,.$$

To the best of our knowledge, there is no result on the eigenvalue θ_μ, for both these processes (and actually for none process except the Brownian motion with a constant drift). Then, in the following subsection, we shall use a Fleming-Viot type algorithm to compute numerically this value (see Section 5.2 for further details).

5. Numerical studies.

To decipher the importance of the attraction in CTL response against a tumor nodule, we illustrate the system (4.1) by some numerical calculations. Hence, we develop simulations in both the Brownian and the reinforced Ornstein-Uhlenbeck models in the biological framework of melanoma tumor nodule (see [CMR$^+$15]).

The goal of this section is thus to determine, in each model described in Equations (4.2), the minimal CTL number leading to nodule eradication, with an initial nodule radius equal to R_0, in both situations. To this end, a classical explicit Euler method is used to find numerical approximations of the solutions of these two systems. For the numerical simulations, we are using the estimated values of the several parameters involved by our models obtained in [CMR$^+$15]. We refer to [CMR$^+$15] and [Chr14] for the statistical methodology used to estimate these parameters. The values of these estimations and the variable definitions are given in Table 2.

Variables	Description	
R_t	nodule radius at t	
E_t	alive part thickness of the nodule at t	
N_t	necrotic part radius of the nodule at t	
A_t	number of alive cells at t	
	(quiescent cells and proliferative cells)	
L_t	scout CTL number at t	
Parameters	Description	Value
n_0	CTL number	variable
μ	killing rate	0.0379 (/min)
λ	tumor cell division rate	0.001 (/min)
d	tumor cell diameter	12.5 μm
r	tumor cell radius	6.25 μm
$\boldsymbol{\delta}$	proliferative part proportion in alive part	0.14
$\boldsymbol{R_{max}}$	maximal radius of the tumor mass at $t = 0$	$100 \cdot 10^2$ μm
$\boldsymbol{R_{min}}$	minimal radius of the tumor mass at $t = 0$	$1 \cdot 10^2$ μm
R_0	tumor mas radius et $t = 0$	$R_0 \in [R_{min}, R_{max}]$
$\boldsymbol{E_0}$	alive part thickness at $t = 0$	$\min(219, R_0)$ μm
N_0	necrotic part radius at $t = 0$	$(R_0 - E_0)$ μm
$\mathbb{E}(\boldsymbol{L_0})$	mean number of scout CTL at $t = 0$	1
$\boldsymbol{\nu_{max}}$	maximal attraction strength	$\frac{1}{100}$

TABLE 2. **Variables and parameter values.** Parameters μ, λ, d, r, are fixed using experimental measurements and statistical studies developed in [CMR$^+$15]. Bold parameter values are not revealed in [CMR$^+$15] and require more analysis, which is described in Section 5.1.

5.1. **Choice of the parameter values.** The success or not of CTL response against a tumor nodule depends on the nodule radius at time $t = 0$, namely $R_0 \in [R_{min}, R_{max}]$. Measurements of [CMR$^+$15] are obtained for a mean diameter nodule at time 0 equals to $300\mu m$. Thus, we assume $R_{min} = 100$ μm and $R_{max} = 1$ cm. Of course, there exist nodules with diameter higher than $2cm$, but we believe that R_0 varying between 100 μm to 1 cm gives an overview of the behavior of the interaction between CTL and tumor nodule. Consequently, we have chosen to fix $\boldsymbol{R_{min}} = 10^2\mu m$, and $\boldsymbol{R_{max}} = 10^4\mu m$.

As noted in [CMR$^+$15], the scale of the parameters have to be carefully determined. Note that, a 100 μm scale is a good choice. Indeed, it makes it possible a numerical analysis with a low number of CTL.

The value of the parameters $\boldsymbol{E_0}$ and $\boldsymbol{\delta}$ are not available too. Thus, they are tuned so that the nodule diameter equation fits the experimental results obtained in [CMR$^+$15]. In particular, they are estimated while running Equation (2.5) without any CTL/nodule interaction, *i.e.*, imposing arbitrarily that $\mathbb{E}[L_t] = 0$ for any time t. As an illustration, we found that a reasonnable proporstion for the proliferative part of the alive part of the nodule is approximately $\delta = 0.14$.

The parameter $\mathbb{E}(L_0)$ is the mean scout CTL number at time $t = 0$. Formally, recall that Z_0^i denotes the i^{th} CTL position at time $t = 0$, and CTL trajectories are assumed identically distributed and independent. Then,

$$\mathbb{E}(L_0) = n_0 \mathbb{P}_{\mu_0}(Z_t^1 \in [R_0, R_0 + r]).$$

But, for the sake of simplicity, we assumed that $\mathbb{E}(\boldsymbol{L_0}) = 1$. In the attraction case, it makes it possible to see directly the impact of the attraction.

In the drifted CTL displacement case, a maximal attraction strength parameter has to be calibrate, which corresponds to the value of $\nu_t = \alpha + \beta l_t$ in Equation (4.2), or equivalently to:

$$\forall s > 0, \qquad \mathrm{d}\rho_s = \mathrm{d}B_s + \left(\frac{1}{2\rho_s} - \nu_t \rho_s\right) \mathrm{d}s,$$

Indeed, the distance ρ_s between a CTL and the center of the nodule at time s is larger than R_s, which belongs to $[10^2 \mu m, 10^4 \mu m]$. Biological measurements give a mean CTL velocity equals to $8.66 \mu m/min$. To counterbalance ρ_s, in the drift term, which is thus higher than 100 μm, we assume that $\alpha = 0$ and $\beta = 10^{-3}$, and fix a maximal attraction strength $\boldsymbol{\nu_{max}} = \frac{1}{100}$. It then corresponds to a choice $\nu_t = \beta l_t \wedge \boldsymbol{\nu_{max}}$.

The attraction strength then vary between 0 and $\boldsymbol{\nu_{max}}$. Note that for the simulations we are assuming that $\sigma = 1$, while, for the QSD approximation to be true we should choose a large σ. Indeed, the choice of a very small attraction strength we have done corresponds, up to a simple time change, to this situation because of the very lengthy tumor cell eradication rate λ. In other words, the QSD approximation holds when *the ratio* between the velocity and the rate λ is large.

Algorithm 1: Fleming-Viot type algorithm for computing θ_μ.

Data: N: number of particles. μ_0 be the distribution of the particles at time 0.
δt discretization step size. Radius R

Initialization: $(Z_0^i)_{1 \le i \le N}$ i.i.d. according to μ_0;

Compute the proportion of alive particles: $q_0 = \frac{\sum_{i=1}^N \mathbb{1}_{|Z_0^i| \ge R}}{N}$.

for $t = 0 \dots T_{max}$ **do**

  For each $i \in \{1, \dots, N\}$: upgrade $\tilde{Z}^i_{t+\delta_t}$ from Z^i_t according to Equation (4.2).

  For each new position, define $A_{t+\delta_t}$ the set of alive particles:

$$A_{t+\delta_t} := \left\{ \tilde{Z}^i_{t+\delta_t} \, : |\tilde{Z}^i_{t+\delta_t}| > R \right\}.$$

  Compute the proportion of alive particles $q_{t+\delta_t} = \frac{\mathrm{card}(A_{t+\delta_t})}{N}$.

  Duplicate each killed particle according to a uniform distribution among alive ones:

$$\forall i \in A^c_{t+\delta_t} \qquad Z^i_{t+\delta_t} \sim \mathcal{U}_{A_{t+\delta_t}} \qquad \text{and} \qquad \forall i \in A_{t+\delta_t} \qquad Z^i_{t+\delta_t} = \tilde{Z}^i_{t+\delta_t}.$$

end

Output: Average value of $(-\log(q_t))_{0 \le t \le T_{max}}$.

5.2. **Fleming-Viot type algorithm and QSD.** Since no theoretical value for the rate of convergence in Theorem 4.1 is known, we will approximate this value using numerical simulations. To this end, a Fleming-Viot type particle system is frequently used.

The main difficulty in approximating the QSD is structural: the probability of the event "the process is not yet killed at time s" goes exponentially fast to 0 as s goes to infinity. Hence it is a rare event for which naive Monte-Carlo methods are not well-suited. To overcome this issue, a Fleming-Viot algorithm, introduced by [BHIM96] that uses rebirth, is used. In particular, we refer to the adaptation proposed in [DMM03] for the numerical solving of the Lyapunov exponent of Feynman-Kac semigroup.

It consists in a modification of a Monte-Carlo algorithm, where "killed" particles, *i.e.*, particles that hit the frountier of the domain of interest, are reintroduced in the current population of not killed particles. In a sense, this leads to handle a constant population size of particles. This

method was used by Villemonais in the framework of QSD. We refer to [Vil13] for the precise assumptions needed to use his algorithm. For reflected processes as we are looking at, it is easily seen that these assumptions are satisfied. The algorithm used for solving the eigenvalue problem is given in Algorithm 1.

Assuming the existence of the QSD and that the convergence of the Fleming-Viot type holds, our aim is to compute θ_μ in Theorem 4.1. If we handle a large number N of particles, we can then approximate θ_μ with:

$$\hat{\theta}_\mu = -\frac{1}{T}\sum_{t=1}^{T_{max}} -\log(q_t),$$

where q_t is the proportion of alive (non absorbed) particles in our simulations.

At last, since we need to estimate the key parameter θ_μ for several values of R, we used Algorithm 1 for a regularly spaced grid of values of R, and then used a non-parametric kernel estimator of θ_μ to obtain the desired eigenvalue, whatever $R > 0$ may be. Complementary numerical insights are given in [Chr14].

5.3. **Numerical results under self-governing CTL displacements.** We first study from a numerical point of view the joint evolution of Equation (4.1) when the dynamics of the particles is described with the Bessel generator $\mathcal{L}$ (radial Brownian motion):

$$\mathcal{L} = \mathcal{L}_t = \frac{1}{2}\sigma^2\partial^2_{yy} + \frac{\sigma^2}{2y}\partial_y$$

The behavior of the solutions is analysed for two initial size of tumor nodule. Figure 3 presents some experiments for $R_0 = 1cm$ and Figure 4 for $R_0 = 1mm$. In each situation, we vary the number of CTL, which is denoted n_0. We also provide in Figure 5 the result of the probability of success of the CTL population in the self-governing Brownian case when $R_0 \in [R_{min}, R_{max}]$ and n_0 varies between 0 and 10^5.

First, as observed in the first lines of Figures 3 and 4, an exponential growth of the nodule occurs when the number of CTL n_0 is too small, leading to an exponential proliferation of the tumor nodule. Second, even though not surprising, it is worth saying that the minimal number of CTL needed for tumor eradication increases with the initial size of the nodule: 10^4 CTL yields tumor eradication when $R_0 = 1mm$ (see last line of Figure 4), and the same number of CTL is not enough to defeat a tumor nodule when $R_0 = 1cm$.

The third columns of Figures 3 and 4 show that the number of arrivals of CTL on the nodule frontier varies linearly with t, and is stationnary as soon as the tumor nodule is destroyed.

At last, we observe in Figure 5 (A), a phase transition in the CTL number leading to tumor eradication. In particular, it is possible to experimentally describe the dependency between the minimal CTL number leading to nodule eradication and the initial nodule radius R_0. This dependency is shown in Figure 5 (B) and seems to be linear. We obtained the following approximation of the phase transition: the minimial number of CTL is given by $n_0^{minimal} = 336R_0 + 1663$, where R_0 is the initial nodule radius expressed in mm.

5.4. **Numerical results under biased CTL displacements.** This situation corresponds to a simulated immunotherapy with chemotactism described in Equations (4.1) with

$$\mathcal{L} = \mathcal{L}_t = \frac{1}{2}\sigma^2\partial^2_{yy} + \left(\frac{\sigma^2}{2y} - (\beta l_t \wedge \nu_{\max})\right)\partial_y,$$

which is a particular case of the self-interacting drifted particles system with $\alpha = 0$. We also have chosen to use a very mild attraction parameter $\beta = 10^{-3}$ with a bounded range at $\nu_{\max} = 10^{-2}$. Our results are summarized in Figures 6 and 7. Let us briefly comment the numerical results obtained in this case. Of course, the conclusions about the monotonicity phenomena observed without simulated immunotherapy remain valid. The striking point concerns the impact of a very mild attraction parameter on the global rate of success of the CTL population. Indeed, when the tumor size is initially $1cm$, we can observe in Figures 3 and 6 that $n_0 = 10^4$ CTL is likely to lead to a loss without self-interacting attraction and to a success with simulated immunotherapy. A phase transition is still observed when looking at the variation of this probability of success when n_0 and R_0 vary. Nevertheless, Figures 5 and 7 prove that the minimal number of CTL is largely improved in the case of simulated immunotherapy: the phase transition occurs for significantly smaller values of n_0 in Figure 7. Moreover, it is also possible to quantitatively describe the dependency of $n_0^{minimal}$ with respect to R_0: this number approximately evolves as:

$$n_0^{minimal} = \mathbb{1}_{R_0 \geq 1.1cm} (3R_0 + 370) + \mathbb{1}_{R_0 \leq 1.1cm} (30R_0 + 70) .$$

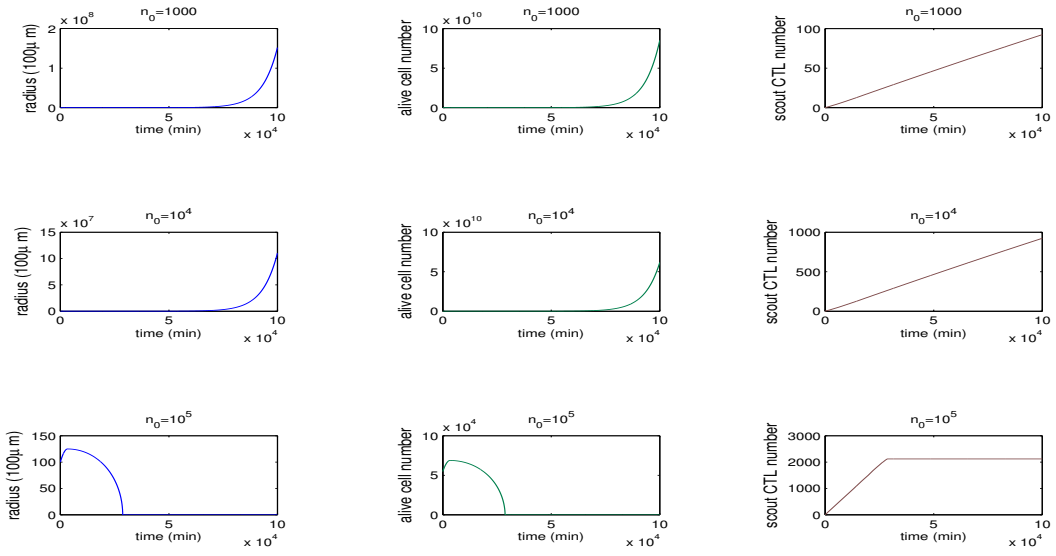

FIGURE 3. **Left:** nodule radius. **Middle:** number of alive cells. **Right:** Number of scout CTL. **First line:** $n_0 = 10^3$ corresponds to around 4.5 alive tumor cells against 1 CTL. **Second line:** $n_0 = 10^4$. **Third line:** $n_0 = 10^5$. The tumor nodule initial size is $R_0 = 1\ cm$ in both experiments and the population of CTL evolves without attraction of CTL, under self-governing dynamics.

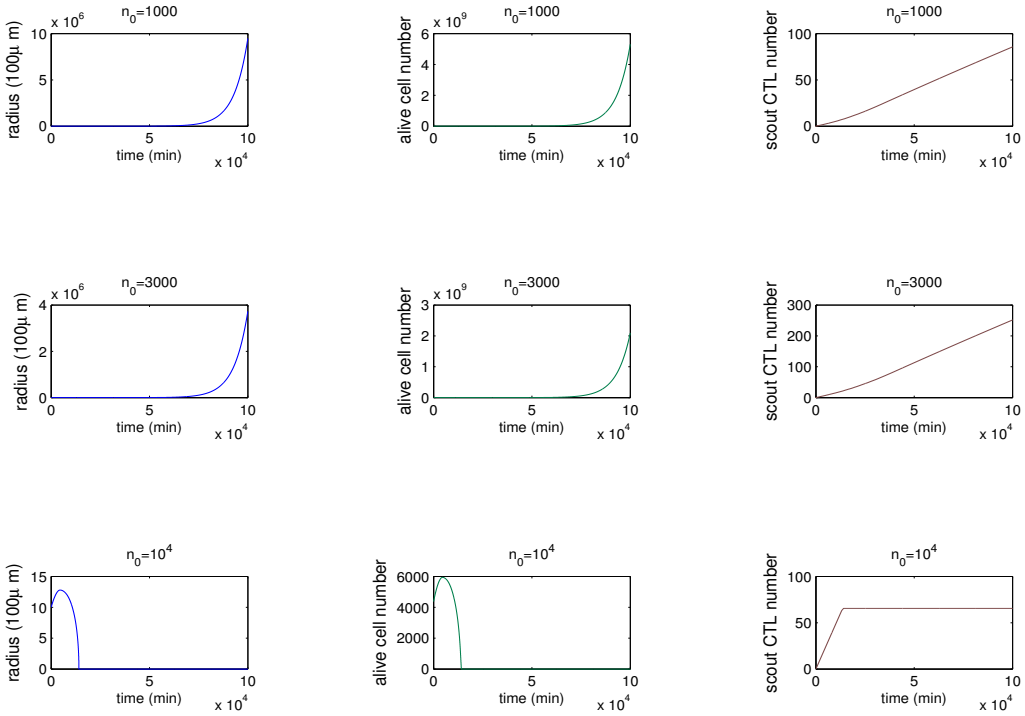

FIGURE 4. **Left:** nodule radius. **Middle:** number of alive cells. **Right:** Number of scout CTL. **First line:** $n_0 = 10^3$ corresponds to around 4.5 alive tumor cells against 1 CTL. **Second line:** $n_0 = 3.10^3$. **Third line:** $n_0 = 10^4$. The tumor nodule initial size is $R_0 = 1\ mm$ in both experiments and the population of CTL evolves without attraction of CTL, under self-governing dynamics.

5.5. **Future developments.** In this paper, we have seen the practical interest of a simulated immunotherapy that induces a self-interacting attraction among the CTL population from a numerical point of view. Nevertheless, many open questions remain opened at this stage. From a theoretical point of view, the study of the well-posedness of the processes involved in this paper seems a challenging task. More interesting would be the derivation of a closed-form equation of the probability of success of the CTL population in both situations of unbiased or self-biased CTL dynamics. From a statistical point of view, the estimation of many parameters described in this paper (mainly the attraction parameter β) seems to be very important to build a success rate. At last, from a practical point of view, it would be very stimulating to understand what kind of biological covariates could be correlated to chemokines and how such a strategy could be implemented to enhance immune system response against tumor nodule.

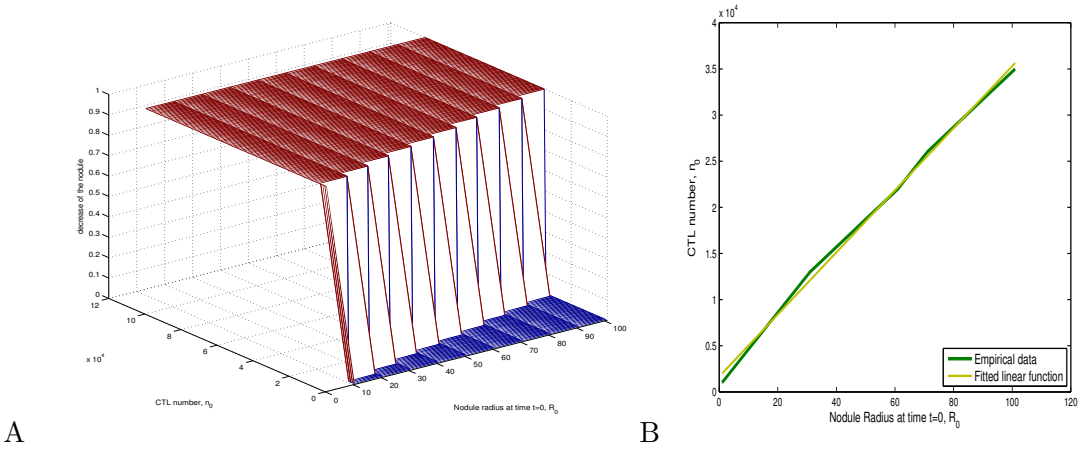

A B

FIGURE 5. **Probability of success of the CTL population versus the nodule growth, according to n_0 (initial number of CTL) and R_0 (initial size of the nodule) in μm.** The dynamics involved by the particle system does not use any self-interacting attraction. (A) A value near to 1 indicates an almost certain success of the CTL population. (B) Minimal number of CTL leading to the nodule eradication, according to the initial size of the nodule radius R_0.

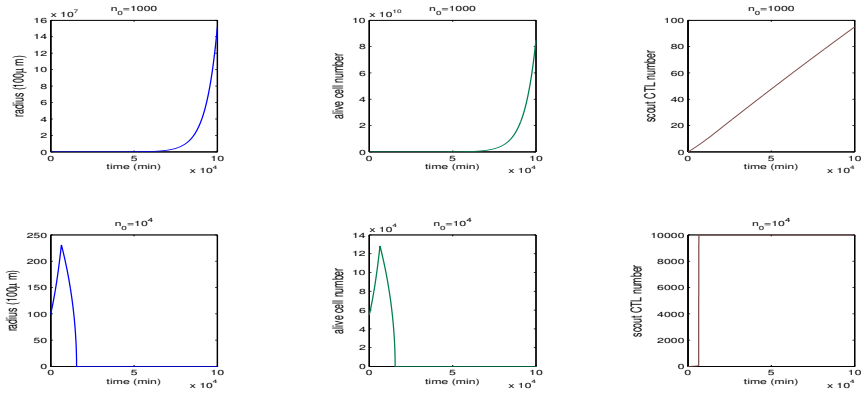

FIGURE 6. **Left:** nodule radius. **Middle:** number of alive cells. **Right:** Number of scout CTL. **First line:** $n_0 = 10^3$ corresponds to around 4.5 alive tumor cells against 1 CTL. **Second line:** $n_0 = 10^4$. The tumor nodule initial size is $R_0 = 1$ cm in both experiments and the population of CTL evolves with a self-reinforced biased dynamics.

REFERENCES

[BdSLY+15] R. Barreira da Silva, M. Laird, N. Yatim, L. Fiette, M. Ingersoll, and M. Alber. Dipeptidylpeptidase 4 inhibition enhances lymphocyte trafficking, improving both naturally occurring tumor immunity and immunotherapy. *Nature Immunology*, 16:850?858, 2015.

[BHIM96] K. Burdzy, R. Holyst, D. Ingerman, and P. March. Configurational transition in a Fleming-Viot-type model and probabilistic interpretation of laplacian eigenfunctions. *Journal of Physics A: Mathematical and General*, 29(11):2633, 1996.

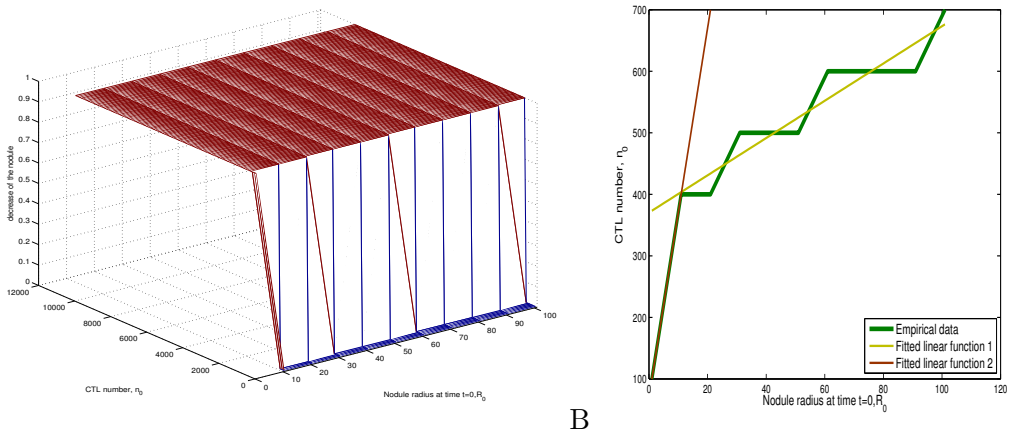

A B

FIGURE 7. **Probability of success of the CTL population versus the nodule growth, according to n_0 (initial number of CTL) and R_0 (initial size of the nodule) in μm.** The dynamics involved by the particle system uses a mild self-interacting attraction. (A) A value near to 1 indicates an almost certain success of the CTL population. (B) Minimal number of CTL leading to the nodule eradication, according to the initial size of the nodule radius R_0.

[BMR13] T. Byczkowski, J. Małecki, and M. Ryznar. Hitting times of Bessel processes. *Potential Anal.*, 38(3):753–786, 2013.

[BS02] A. N. Borodin and P. Salminen. *Handbook of Brownian motion—facts and formulae*. Probability and its Applications. Birkhäuser Verlag, Basel, second edition, 2002.

[Cat87] P. Cattiaux. Régularité au bord pour les densités et les densités conditionnelles dune diffusion réfléchie hypoelliptique. *Stochastics and Stoch. Rep.*, 20:309–340, 1987.

[Cat91] P. Cattiaux. Calcul stochastique et opérateurs dégénérés du second ordreII. problème de dirichlet. *Bull. Sciences. Math.*, 115:81–122, 1991.

[CFP+09] I. Caramalho, M. Faroudi, E. Padovan, S. Müller, and S. Valitutti. Visualizing CTL/melanoma cell interactions: Multiple hits must be delivered for tumour cell annihilation. *Journal of cellular and molecular medicine*, 13(9b):3834–3846, 2009.

[Chr14] C. Christophe. Modélisation aléatoire de l'activité des Lymphocytes T Cytotoxiques. PHD Thesis. Université de Toulouse., 2014.

[CM02] P. Cattiaux and L. Mesnager. Hypoelliptic non-homogeneous diffusions. *Probab. Theory Related Fields*, 123(4):453–483, 2002.

[CM10] P. Cattiaux and S. Méléard. Competitive or weak cooperative stochastic Lotka-Volterra systems conditioned to non extinction. *J. Math. Biology*, 60(6):797–829, 2010.

[CMR+15] C. Christophe, S. Müller, M. Rodrigues, A. Petit, P. Cattiaux, L. Dupré, S. Gadat, and S. Valitutti. A biased competition model theory of cytotoxic T lymphocyte interaction with tumor nodules. *Plos One*, 2015. Published: March 27, 2015.DOI: 10.1371/journal.pone.0120053.

[CMSM13] P. Collet, S. Martínez, and J. San Martín. *Quasi-stationary distributions*. Probability and its Applications (New York). Springer, Heidelberg, 2013. Markov chains, diffusions and dynamical systems.

[DL10] M. L. Dustin and E. O. Long. Cytotoxic immunological synapses. *Immunological reviews*, 235(1):24–34, 2010.

[DMM03] P. Del Moral and L. Miclo. Particle approximations of Lyapunov exponents connected to Schrödinger operators and Feynman-Kac semigroups. *ESAIM Probab. Stat.*, 7:171–208, 2003.

[GLNÖ98] R.. L. Graham, B. D. Lubachevsky, K. J. Nurmela, and P. R. J. Östergård. Dense packings of congruent circles in a circle. *Discrete Math.*, 181(1-3):139–154, 1998.

[GMBdB14] S. Gadhamsetty, A. F. M. Marée, J. B. Beltman, and R. J. de Boer. A general functional response of cytotoxic T lymphocyte-mediated killing of target cells. *Biophysical journal*, 106(8):1780–1791, 2014.

[HBC+12a] T. Harris, E. Banigan, D. Christian, C. Konradt, W. Tait, K. Norose, E. Wilson, B. Johnn, W. Weninger, A. Luster, A. Liu, and C. Hunte. Generalized lévy walks and the role of chemokines in migration of effector cd8+ t cells. *Nature Letter*, 486(1):545–548, 2012.

[HBC+12b] T. H. Harris, E. J. Banigan, D. A. Christian, C. Konradt, K. Wojno, E. D. Norose, E. H. Wilson, B. John, W. Weninger, A. D. Luster, et al. Generalized lévy walks and the role of chemokines in migration of effector cd8+ t cells. *Nature*, 486(7404):545–548, 2012.

[HM13] Y. Hamana and H. Matsumoto. The probability distributions of the first hitting times of Bessel processes. *Trans. Amer. Math. Soc.*, 365(10):5237–5257, 2013.

[IW81] N. Ikeda and S. Watanabe. *Stochastic differential equations and diffusion processes*, volume 24 of *North-Holland Mathematical Library*. North-Holland Publishing Co., Amsterdam-New York; Kodansha, Ltd., Tokyo, 1981.

[KTHI+00] A. R. Kansal, S. Torquato, G. R. Harsh Iv, A. E. Chiocca, and T. S. Deisboeck. Cellular automaton of idealized brain tumor growth dynamics. *Biosystems*, 55(1):119–127, 2000.

[LYW+15] B. Lin, T. Yin, Y. Wu, T. Inoue, and A. Levchenko. Interplay between chemotaxis and contact inhibition of locomotion determines exploratory cell migration. *Nature Communications*, 6(6619), 2015.

[MDP06] D. G. Mallet and L. G. De Pillis. A cellular automata model of tumor-immune system interactions. *Journal of Theoretical Biology*, 239(3):334–350, 2006.

[MV12] S. Méléard and D. Villemonais. Quasi-stationary distributions and population processes. *Probab. Surv.*, 9:340–410, 2012.

[PB82] A. S. Perelson and G. Bell. Delivery of lethal hits by cytotoxic T lymphocytes in multicellular conjugates occurs sequentially but at random times. *The Journal of Immunology*, 129(6):2796–2801, 1982.

[RMJM78] T. L. Rothstein, M. Mage, G. Jones, and L. L. McHugh. Cytotoxic T lymphocyte sequential killing of immobilized allogeneic tumor target cells measured by time-lapse microcinematography. *The Journal of Immunology*, 121(5):1652–1656, 1978.

[RY99] D. Revuz and M. Yor. *Continuous martingales and Brownian motion*, volume 293 of *Grundlehren der Mathematischen Wissenschaften [Fundamental Principles of Mathematical Sciences]*. Springer-Verlag, Berlin, third edition, 1999.

[SOS11] R. D. Schreiber, L. J. Old, and M. J. Smyth. Cancer immunoediting: integrating immunity's roles in cancer suppression and promotion. *Science*, 331(6024):1565–1570, 2011.

[SSTT07] M. Sanz-Solé and I. Torrecilla-Tarantino. Probability density for a hyperbolic spde with time dependent coefficients. *ESAIM Probab. Stat.*, 11:365–380, 2007.

[Vil13] D. Villemonais. General approximation method for the distribution of markov processes conditioned not to be killed. *arXiv:1106.0878v3*, 2013.

[WDFV06] A. Wiedemann, D. Depoil, M. Faroudi, and S. Valitutti. Cytotoxic T lymphocytes kill multiple targets simultaneously via spatiotemporal uncoupling of lytic and stimulatory synapses. *Proceedings of the National Academy of Sciences*, 103(29):10985–10990, 2006.

[WL10] N. Watari and R.G. Larson. The hydrodynamics of a run-and-tumble bacterium propelled by polymorphic helical flagella. *Biophysical Journal*, 98(1):12–17, 2010.

Patrick CATTIAUX, Institut de Mathématiques de Toulouse. CNRS UMR 5219., Université Paul Sabatier, 118 route de Narbonne, F-31062 Toulouse cedex 09.

E-mail address: cattiaux@math.univ-toulouse.fr

Claire CHRISTOPHE, Laboratoire de Mathématiques Jean Leray, CNRS UMR 6629., Université de Nantes, 2 rue de la Houssinière, BP-92208, F-44322 Nantes Cedex 3.

E-mail address: claire.christophe@univ-nantes.fr

Sébastien GADAT, Toulouse School of Economics, Manufacture des Tabacs, Université Toulouse 1 Capitole, 21 alle de Brienne, F-31000 Toulouse.

E-mail address: sebastien.gadat@tse-fr.eu